Development of Carbon Nanofiber Reinforced HNBR Composite for Sealing Applications

A Thesis

Presented to

the Faculty of the Department of Mechanical Engineering

University of Houston

In Partial Fulfillment

of the Requirements for the Degree

Master of Science

in Mechanical Engineering

by

Yang Sun

December 2014

Development of Carbon Nanofiber Reinforced HNBR Composite for Sealing Applications

Yang Sun

Approved:

Chair of the Committee
Li Sun, Associate Professor
Mechanical Engineering

Committee Members:

Cunjiang Yu, Assistant Professor
Mechanical Engineering

Jiming Bao, Assistant Professor
Electric Engineering

Suresh K. Khator, Associate Dean,
Cullen College of Engineering

Pradeep Sharma, Professor and Cullen
Chair, Mechanical Engineering

Acknowledgements

I would like to express my deepest thanks to my advisor, Dr. Li Sun, for his aspiring guidance, genuine encouragement and tireless support during the performance of this research. Your advice on both research as well as on my career have been priceless.

I am also grateful to my committee members, Dr. Cunjiang Yu and Dr. Jiming Bao for serving as my committee members. I also want to thank them for letting my defense be an enjoyable moment, and for their brilliant comments and suggestions.

I would also like to thank Yanan Hou, Christopher Ortega, Sicong Sun, and other members of Dr. Sun's group.

Financial assistance from GE Inc. is also gratefully acknowledged.

Development of Carbon Nanofiber Reinforced HNBR Composite for Sealing Applications

An Abstract

of a

Thesis

Presented to

the Faculty of the Department of Mechanical Engineering

University of Houston

In Partial Fulfillment

of the Requirements for the Degree

Master of Science

in Mechanical Engineering

by

Yang Sun

December 2014

Abstract

Carbon nanofiber(CNF) as a novel filler has been studied by researchers with huge enthusiasm owe to its special properties, like light weight, sustainability of large deformation, chemical stability, corrosion and fatigue resistance, vibration and noise reduction capability, especially in rubber reinforcement. In this paper, cost effective carbon nanofibers (CNFs) are used as nanofillers in order to improve processing control and reproducibility for large scale engineering applications. Hydrogenated nitrile butadiene rubber (HNBR) is used as rubber matrix, for its outstanding performance in mechanical durability and chemical stability. Processing, microstructure, mechanical and thermal properties of HNBR have been studied along with nanofillers, CNFs and other conventional fillers, carbon black and silica. Mechanical measurements and microstructure analysis show that interfacial debonding happens in the hybrid-filler composites. The results indicated that the compatibility of CNF and conventional fillers is good and the modulus achieves highest at the cost of low elongation at certain ratio.

Table of Contents

List of Figures

List of Tables

Chapter 1 Introduction

Filler-reinforced polymer-matrix composites have been extensively used in practical applications for a long time owing to their superior properties. With the fast development in nanoscience and nanotechnology, there is growing interests in introducing nano-scale fillers to polymers, with the hope of further modify and improve polymer properties utilizing the nano-effects. In the meanwhile, such attempts also stimulate theoretical studies on revealing the interactions between the filler and matrix since the structure-property correlation is not well known in nanocomposite materials.

There are many different types of ploymer with different physiochemical properties, processing and manufacturing procedures and applications. In this study, we focus on rubber elastomers. Due to their low cost and widely tunable properties, rubber can find applications from tires, to belts to seals etc. However, natural or pure synthetic rubbers cannot be directly made into products and reinforcing fillers are always necessary to bring their performance up to specific requirements[1-5]. Currently, most common fillers used for rubber are carbon black and silica particles. Thus indeed the rubber products we use today are made from composite materials.

By combining two or more different types of materials with distinct properties together, the composites can not only incorporate the desirable properties of different materials but more often obtain enhanced performances that cannot be achieved by any individual components. Many of the nano- effects are not well understood due to the complex nature of material interactions at the small scale. With the discovery of

increasing fascinating properties in composite materials, such as light weight, superior mechanical properties, fatigue/corrosion resistance and low manufacturing and maintenance cost, their potential engineering applications in aerospace, automobile, marine, civil, electronic, sporting, medical and leisure equipment have attract growth scientific and industrial interests.

A wide variety of fillers have been introduced to modify rubber matrices, carbon black is actually nanoscale filler, and it is an amorphous form of carbon with large variations in sizes. More recently, other nano-scale fillers such as the nanoclay, nanoparticles, nanorods/nanowire and carbon nanotubes have been tested and show promising property enhancement to the rubber due to their special size, shape and interface-related characteristics[6, 7]. With large surface-area-to-volume ratio, nanomaterials can introduce strong interaction between the matrix and the stiffer phase, and they can also affect polymerization and molecule configuration of the matrix material.

Currently used carbon black and silica particle fillers when compounded with rubber shown greatly improved mechanical properties, such as strength, modulus and abrasion resistance[8-10]. With the cost of other carbon nanomaterials dropping at an accelerating speed and their availability fast expanding fillers like the multiwall carbon nanotubes (MWNTs) and carbon nanofibers (CNFs) are finding their way into engineering applications[11, 12]. However, as indicated by many studies, adding small size fillers into polymers always facing challenges in achieving uniform distribution and materials processability. Carbon black and silica particles are mixed with rubber matrix by mechanical compounding. But due to the high aspect ratio of one-dimensional MWNT and CNF, dispersion of these highly anisotropic and sometime entangled nano-scale

fillers in a solid phase matrix can be difficult. Thus the nanofiller dispersion, in addition to interfacial bonding, becomes the biggest challenges in composite manufacturing and product development.

In this study, we focus our research on the synthesis, microstructure analysis and mechanical properties characterization of hybrid-filler HNBR composites. We first studied the CNF reinforced polymer properties and then moved onto the use of CNF fillers together with conventional carbon black and silica fillers to compare the reinforce effects of different fillers. The use of hybrid-fillers allows a wider range of HNBR properties modification and more importantly will help improving material process ability and optimizing cost effectiveness.

The organization of this thesis is as follows: Chapter 1 is introductory; Chapter 2 summarizes the recent progresses on nano-technology as well as polymer science. Chapter 3 addresses the specific objectives of the research and the detailed scope of the work. Chapter 4 describes the details of experimental methods and techniques used in the research. Chapter 5 shows the experimental results and analysis. Important conclusions derived from the study are given in Chapter 6.

Chapter 2 Literature Review

Mechanical and thermal properties are two of the most studied composite characteristics due to both their scientific and application importance. A composite is defined as a material that is composed of two or more materials, which normally have totally different physical or chemical properties. Usually, depending on the existence form, materials in composite can be distinguished as the base component and the reinforcing components. The base material is usually the majority component and normally forms a continuous phase and the reinforcing material usually is dispersed in the base material matrix. The most simplified model describes the composite mechanical properties by using the sum of properties of each component weighted by the volume fraction of that component[13]. This model can provide estimations to the properties of conventional macroscale composites, where the interface effect is not significant and the interactions between components have minimum impact on the component performance. However, these assumptions often fail in nanocomposites, in which composite properties are often not linearly dependent on the component fraction. In most of such cases, interface and material interactions will allow the nanocomposites to not only maximize desired properties from all the ingredients, but also introducing new properties that are not possessed by individual components. On the other hand, there are also possible issues with material compatibility, filler dispersion and interfacial bonding when forming composites, these issues will cause significant problems and with materials deterioration. Also for practical engineering application and product manufacturing of nano-composite, the additional cost, reproducibility, compatibility of current techniques are also of critical

importance. In this research we investigated the effects of different types of fillers to the mechanical properties of HNBR for sealing application. The nanofillers are introduced together with conventional fillers to reduce cost and more importantly improve the dispersion of fillers. So far, there is very limited information on composites with hybrid-fillers the literature and our study provides the some insight into how to composite materials can take advantage of fillers with different size and shape to achieve improved performances. These high performance HNBR composites can have extensively applications in oil and gas industries where the requirements on the mechanical performances, thermal stability and chemical stability continue to increase.

2.1 Nano-scale Materials Science and Technology

2.1.1 The Rise of Nanotechnology

The concepts that seeded nanotechnology were first discussed in 1959 by the renowned physicist Richard Feynman in his American Physical Society (APS) talk entitled "There's Plenty of Room at the Bottom"[14]. He suggested that it should be possible to make nanoscale machines by arranging the atoms the way we want. He also mentioned that scaling issues would be significant for the relative strength of various forces would change. With two nano-technology related challenges raised up, tiny motor and small letters, the talk inspired the conceptual beginnings of the field decades later. The term "nano-technology" is first used by Norio Taniguchi in 1974[15], though it was not widely known. Not until the 1980s, emergence of nanotechnology as a field occurred and bloomed caused by the convergence of experimental advances such as the invention of the scanning tunneling microscope in 1981 and the discovery of fullerenes in 1985, with

the elucidation and popularization of a conceptual framework for the goals of nanotechnology beginning with the 1986 publication of the book Engines of Creation by nanotechnology pioneer Eric Drexler, which predicts the future achievements of nanotechonology in medicinal, biological and mechanical engineering field. Since the 1980s, technology of manipulating, control and fabricating small structures and devices had advanced dramatically, initially led by the electronic industry and then followed by physics, chemistry, many disciplines in engineering and technology and also biomedical sciences. Many milestones in fabrication and science at the nanoscale have been achieved. One such example is that on Sep 28th, 1989, D. Eigler, a physicist and an IBM Fellow at the Almaden Research Center, succeeded in writing letters "I-B-M" using 35 individual xenon atoms on a nickel (110) surface using an STM. This is the first time for mankind to build small structures by manipulating individual atoms with atomic-scale precision. Since 2000s, we have seen dramatic increase in funding, publication and reports on nanoscience and nanotechnology. Now we can make many different types of materials and structures at nanoscale, it is time to meet the challenges of develop large scale engineering application of these nano-materials and nanotechnology so that their superior properties can be used to improve our everyday life.

2.1.2 History of Carbon Nano-materials

Since our early ancestors first learned to make fires, human have been producing carbon-based materials, and mostly in the form of nanoparticles. The smoke and soot from campfires contained small amount of carbon nanoparticles now known as fullerenes and even the carbon nanotubes, along with many other combustion byproducts in the

form of other carbon structures. But due to the limitation of existing observation and characterization method, these nanostructures were largely overlooked. It is until 1970s, scientists began to be able to produce nano-scale carbon fibers with better control by using chemical vapor deposition method[16]. Ten years later, the first fullerene molecule was discovered by Richard Smalley, et al. which greatly expanded the number of known carbon allotropes. In 1991, S. Iijima, a physical in NEC, showed the clear evidence of the existence of multi-walled carbon nanotubes (MWNTs) in the insoluble material extracted from powders collected from the arc-burned graphite rods using transmission electron microscope (TEM)[17]. Since then, buckyballs and buckytubes have become the subjects of intense research, both for their unique structure and more importantly superior physiochemical properties.

2.1.3 Properties of nano-scale materials

Nanoscale materials can be defined as those whose characteristic length scale lies within the nanometric range, and currently it is generally accepted that any materials with at least one-dimension is smaller than 100nm can be called a nanomaterial. Within this length scale, the properties of matter are sufficiently different from individual atoms or molecules and from bulk materials.

The “nano-effect” becomes significant when the material dimension becomes comparable to the characteristic length of physical parameter. For example, when the optical properties of material are concerned, the wavelength is the characteristic length. Bulk gold appears yellow in color while nanosized gold appears red due to the restriction on the movement of the electrons that gold particles react differently with light, their

color can change from red to purple and green. For mechanical properties of a material, normally the defect structure will have a dominant effect. Nanomaterials with small grain size or unique atomic arrangement can have totally different defect structure and dislocation behaviors to have mechanical properties different from conventional bulk. A good example is the carbon nanomaterials, carbon nanotubes can be 100 times stronger than steel at the same weight, all because of they have the unique atomic structure.

For rubber industry, significant amount of carbon black and silica are used as reinforcing additives to improve product performances. They can be considered as nano-scale materials after ultrasonication as shown in Fig 2.1 and Fig 2.2 Graphs are taken under Transmission Electron Microscope (TEM), the first graph is carbon black and the second one is silica with the scale bar 50nm.

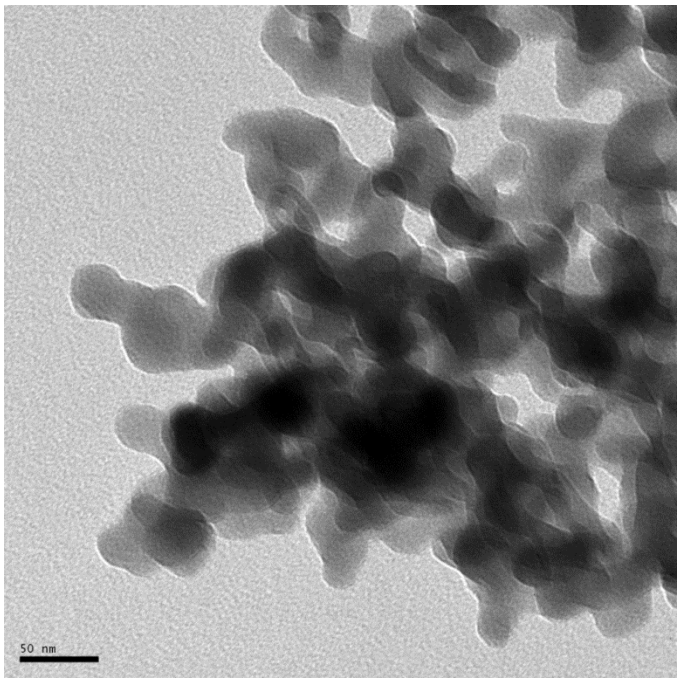

Figure 2.1 Morphology of carbon black

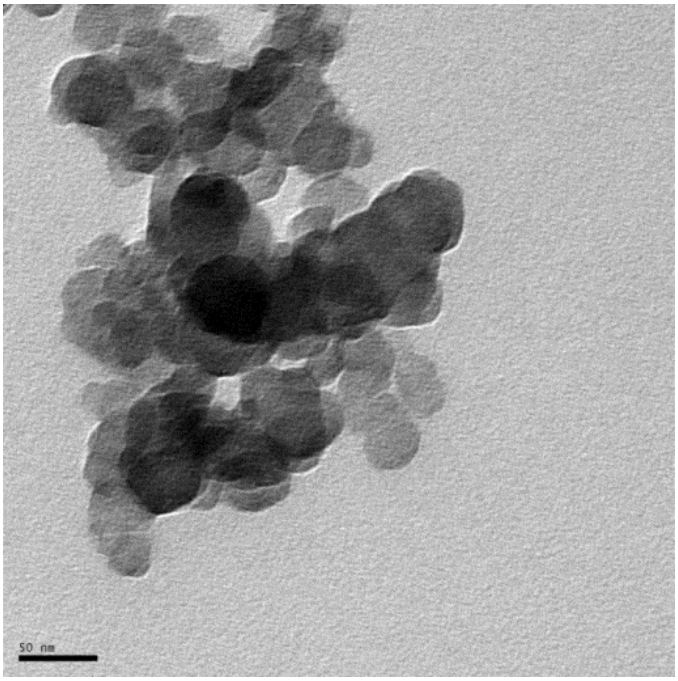

Figure 2.2 Morphology of silica

As mentioned previously, human have familiar with carbon materials for a long time, and with the discovery of more carbon nano-structures in the 1980s, carbon nanomaterials is firstly becoming a new material industry in the new century. With their unique and most of the time superior properties, , carbon nanomaterials are playing an important role for both research study and practical applications. Well-known materials like carbon nanofibers (CNFs), multi-wall carbon nanotubes (MWCNTs) and single-wall carbon nanotubes (SWCNTs) are investigated and their unmatchable mechanical properties like the Young's modulus, strength and resilience have caught the industry attentions for some time. Table 2.1 compares the physical properties of representative carbon nanostructures with conventional engineering materials.

Table 2.1 Physical properties of carbon materials compare with Cu[18-25]

Material	Density (g/cm^3)	Tensile strength (GPa)	Young's modulus (GPa)	Specific Strength	Resistivity (Ω*m)
SWNTs	0.03	50-200	900-1700	1.7×10^{5}-6.7×10^{5}	10^{-6}-10^{-7}
MWNTs	1.3-1.4	11-63	270-950	8.2×10^{3}-4.7×10^{4}	9×10^{-6}
Micro-fibers	1.78-2.15	2-5	80-700	9.3×10^{2}-2.8×10^{3}	1.8×10^{-5}
CNFs	1.8-2.1	2.7-7.0	400-600	1.3×10^{3}-3.9×10^{3}	10^{-5}-10^{-6}
Copper	8.96	0.22	130	24.5	1.72×10^{-8}

2.1.4 Synthesis of Carbon Nano-materials

2.1.4.1 Synthesis of Buckminsterfullerene

Buckminsterfullerene (C_{60}) was first generated in 1985 by Harold Kroto, Robert Curl and Richard Smalley[26] by laser evaporation of graphite, however, the early yield of these nanomaterials was very low and the C_{60} are mixed with many other carbon products. This technique was improved later but still limited to laboratory research. Not until the 1990s, W. Krätschmer and D. R. Huffman[27] developed a simpler and more efficient method of producing fullerenes with much high yield, which boosted the fullerene research significantly. In this technique, two high-purity graphite electrodes are used and after igniting an arc discharge between the two electrodes, black soot can be produced in large quantity. Fullerenes can be extracted from the soot in polymer solution using chromatography.

2.1.4.2 Synthesis of Carbon Nanotubes (CNTs)

Report on the fabrication and observation of one-dimensional carbon nanostructures can be back dated to 1880s with fabrication of carbon filament, there are few later reports showing such carbon structures. Hughes and Chambers proposed a method for growing

carbon filaments from ‘swamp gas’ in U.S.patent 405.480 in 1889[28]. In 1953, W. R. Davis, R. J. Slawson and G. R. Rigby was able to observe two twisted carbon fiber together in the form of a rope which diameter is in nanoscale for the first time[29]. But due to the lack of controlled synthesis and more importantly, characterization techniques, now we most accredit the carbon nanotubes (CNTs) discovery to Iijima in 1991, which provided unequivocal proof of the existence and structure of MWNTs, when he studied products from a new arc evparation method developed for producing C_{60} using TEM. In 1993, the same group reported the discovery of SWNTs.

After 25 years of study and development, different synthesis methods can now be used to produce controlled carbon nanostructures. Among these methods, arc discharge, laser ablation and chemical vapor deposition are commonly used in recent world.

Arc discharge

Arc discharge generates a high temperature (above 1700 ˚C) for CNT formation[30]. A schematic graph of this technique is represented in Figure 2.3. Multi-wall nanotubes (MWNTs) production using arc discharge synthesis is relative very simple once all conditions are ensured. This process is often conducted in a chamber filled with helium at subatmospheric pressure with two graphite electrodes. MWNTs are formed using a DC arc discharge. During this process, the two charged-graphite electrodes are momentarily brought into contact to start the arc and then separated with sustained arc discharge to maintain carbon evaporation from anode. Normally the MWNTs can be produced even without any catalyst, but transition metal catalysts cannot only improve the MWNT yield but they are necessities for producing single wall nanotubes (SWNTs)[31]. The catalysts, in

the form of nanoparticles are usually mixed with graphite in electrode manufacturing. During CNT production, a constant gap distance between the electrodes is maintained to ensure the stability of current density and a constant anode consumption rate.

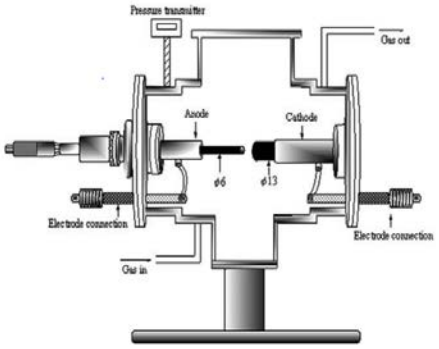

Figure 2.3 Schematic of arc discharge apparatus

Laser ablation

Laser ablation technique has also been developed for CNT production. This method removes carbon atoms from a solid surface by irradiating it with a high power laser beam. The first report using laser ablation to produce SWNTs from a block of pure graphite appeared in 1996[32]. A schematic apparatus picture is shown in Figure 2.3. The raw block material use as ablation target is a mixture of graphite powder, carbon cement and metal catalysts. After placing it in a heated cylindrical mold and baking for several hours for solidification, this graphite block is placed in a transparent tube first pumped down and then filled with argon gas, The tube was inserted inside an furnace with a laser beam pointed at the graphite target to introduce carbon evaporation, a cold finger was used to collect carbon products. Carbon nanotubes will normally form when the laser ablates the target with a furnace temperature of approximately 1200□C. The properties of the obtained CNTs strongly depends on a number of parameters such as the laser

wavelength, the structural and chemical composition of the target material, the chamber pressure as well as substrate temperature. High yield and improved CNT purity can be achieved using this ablation method, but nanotubes entanglement can be an issue for this method.

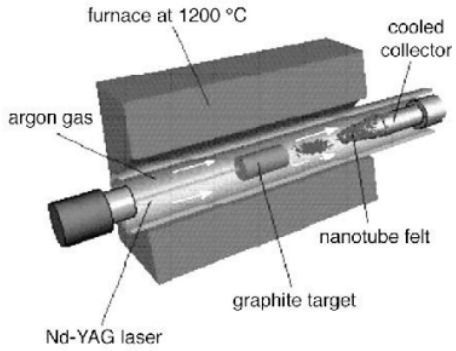

Figure 2.4 Classic laser ablation technique

Chemical vapor deposition (CVD)

With the development of CNT synthesis technology, catalytic chemical vapor deposition becomes the standard method for CNTs product. Initially this method was used for producing carbon filaments from the catalytic decomposition of carbon-containing gas over metal surfaces, after a long time of modification and improvement and also with better understanding of carbon nanostructure growth, this technique succeeded in being applied to synthesizing carbon nanotubes first by Yacamàn et al[33]. With fast development in this field, CVD is considered to be the only economically viable process for large-scale CNT production. This technique is carried out in a flow furnace at atmospheric pressure with catalysts inside. Inert gas mixed with hydrocarbon flows over the catalyst bed at temperatures from 500 ˚C to 1100 ˚C.

Hydrocarbon gas decomposes on the catalytic nanoparticles to form CNTs in the chamber. Fig 2.5 shows the schematic of a thermal chemical vapor deposition process which requires a relatively high synthesis temperature. Other efforts implementing plasma to lower reaction temperature have also been succeeded and thus developed the so-called plasma enhanced chemical vapor deposition (PECVD)[34]. Synthesis temperature can be lower down to 100 ˚C. During this process, strong electric field is induced by plasma thus the growth direction of carbon nanotubes can also be controlled. Fig 2.6 shows the process how carbon nanotubes grow in PECVD.

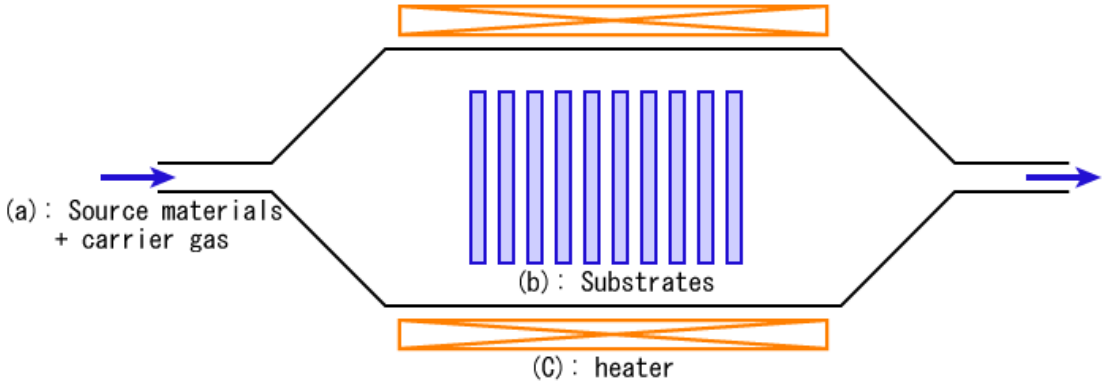

Figure 2.5 Schematic of thermal chemical vapor deposition

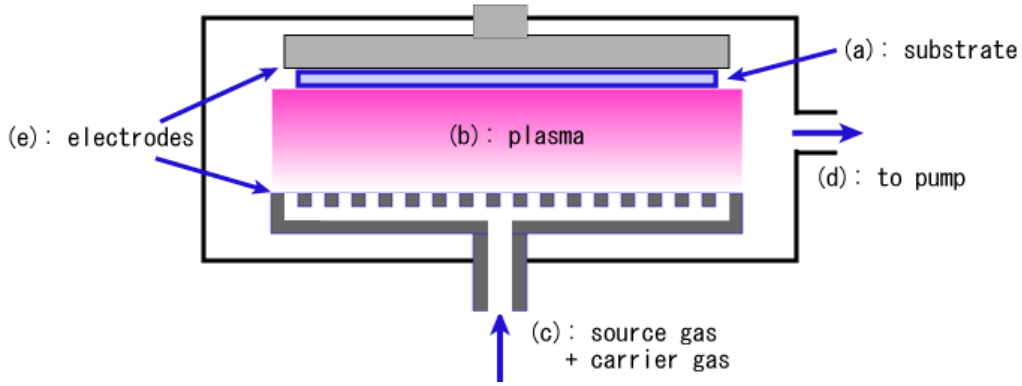

Figure 2.6 Schematic of plasma enhanced chemical vapor deposition

2.1.4.3 Synthesis of Carbon Nanofiber (CNFs)

Nano-carbon with tubular microstructure is called tubes and with solid cylindrical structures is called the filament or fiber. Carbon nanofibers have similar structure as the MWNTs so have also drawn lots of attention for their thermal, electrical, and mechanical properties. For synthesis, catalytic chemical vapor deposition (CCVD) is the dominant commercial technique for the production of so-called vapor grown carbon nanofibers (VGCNFs)[35]. Fig 2.7 shows the schematic production process used by Applied Sciences, Inc. in producing VGCNFs.

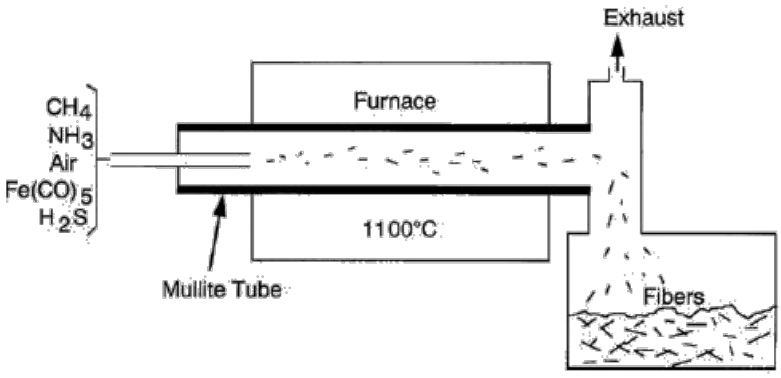

Figure 2.7 VGCNFs production schematic shown by Applied Sciences, Inc

2.2 Polymer Science

2.2.1 History of Polymer

The history of people living with polymeric materials can be traced back to thousands of years ago, but provided by nature. Not until the year 1833 were people able to synthesize such materials and named it “polymer”. The meaning of this term “polymer” at that time is different from what we perceive today. In his designation, the term “polymer” means if two substances have empirical formulae that can be integer multiples

of each other[36]. In 1920, Hermann Staudinger proposed the concept of polymers in the sense we are using today. In his land mark paper "Über Polymerisation"[37], he claimed that rubber and other polymers such as starch are long chains of short repeating molecular units linked by covalent bonds as shown in Fig 2.8.

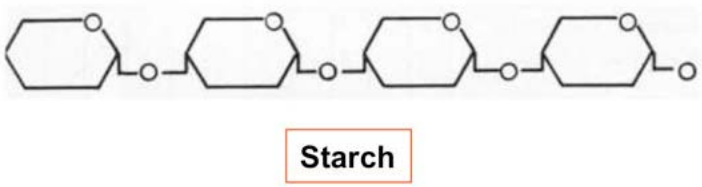

Figure 2.8 Schematic graph of polymer structure of starch

With his pioneering research, properties of synthesized polymers were discovered which astonished the world and greatly promoted the development of polymer industry. As of the decade 1940-1950, polymers were used as substitutes for traditional materials. Due to lack of experience in manufacture, it was belittled for poor quality. Nowadays the universality of polymers is well established. They are present in all fields of industrial products as additive or structural materials. With more and more fascinating properties being found, it is more and more compelling logical that here are no bad polymers, only bad applications of them.

2.2.2 Mechanical Behaviors of Polymer

2.2.2.1 Basic Stress-Strain Relation

The term of mechanical property is commonly used to denote the stress-strain relationship for a material polymer system. In such relationship, modulus, strength and

ductility are a few of the commonly referred to mechanical properties to describe the characteristics of a material.

As far as the material strength is concerned, there is tensile strength as well as compression strength describing the maximum stress a material can sustain under corresponding loading conditions[38]. Most of the materials mechanical properties are measured in the tensile mode using an apparatus called tensile machine such as an Instron machine. In the tensile measurement mode, a “dog-bone” shaped sample is clumped down to the grips of the tensile machine. When the sample is stretched by the machine the corresponding load is recorded. Based on knowing the original dimension of the sample, the engineering stress and engineering strain data can be obtained. Most of tensile machine is operated under the strain control mode, where the sample deformation rate is controlled with loading recorded. Certain machines are also capable of operating under the stress controlled mode where the applied load can be controlled with corresponding stress recorded. Fig 2.9 shows a typical engineering stress-strain curve measured for a sample with medium level strength and ductility, most metals will behave similar to this curve. Upon applying a tensile stress, sample will be stretched along the loading direction and shrink in other two directions. The initial deformation is normally elastic and can be linear. With increasing stress and strain, material will undergo plastic deformation, where crystalline materials, dislocation motion are activated. During plastic deformation, if the true stress and true strain are calculated, a so-call strain hardening process can normally be observed. With the progression of plastic deformation, the engineering stress will show a maximum value, and this is the tensile strength, which indicates the largest load a sample can sustain. After this point, local deformation

becomes dominant where the parts with smaller cross section area will be under higher true stress and resulting in further plastic deformation, this process is shown as necking of local areas. Continuous necking will finally lead to sample failure. While some of the material mechanical characteristics such as the Young's modulus or Poisons 'ratio show weak dependence on the sample shape and microstructure, many other sample mechanical performances such as strength, ductility and toughness can be very different from sample to sample. In practical applications, the material mechanical performances will be impact by design, processing, and surface conditions

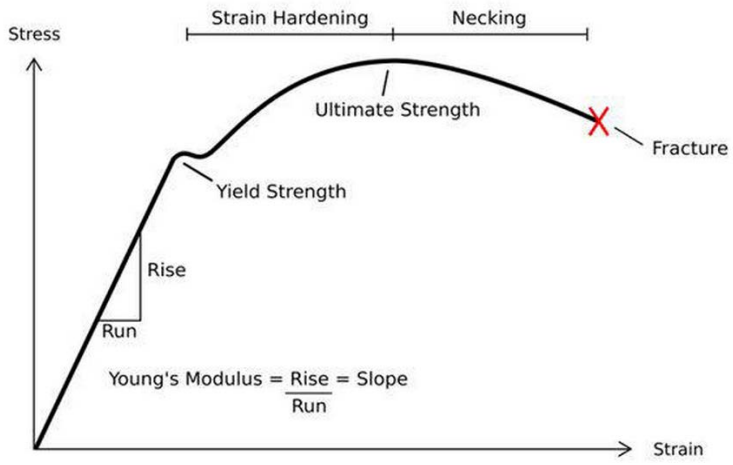

Figure 2.9 Schematic of stress- strain curve

2.2.2.2 Mechanical Relaxation

Mechanical relaxation refers to the phenomenon where a material relieves stress under constant strain or continues to deform under constant stress. For polymers, relaxation is inherent and an important characteristic mechanical response. This time depend deformation behavior is also called viscoelasticity[39]. Stress variation during relaxation is non-linear and can be expressed as

$$\sigma(t) = \sigma_0 e^{-t/\tau}, \tag{2.1}$$

where σ_0 is the initial stress and τ is the relaxation time.

Stress relaxation is a reflection of the motion of polymer molecule chain under external load. When the motion of polymer chains is restrained, then the relaxation effect will be smaller. As shown in Fig 2.10a, comparing the cross-linked polymer and linear polymer, the stress relaxation in the previous when will be smaller than the latter one since the motion of polymer chains will be much more limited in the three-dimensionally cross-linked polymer. As for the same polymer in different states, they will also have different stress relaxation behaviors. As shown in fig 2.10b, the same polymer materials can also show changing stress relaxation behavior due to molecular structure change, this change can be manipulated by temperature. For polymers in the glass state at low temperature, the compression relaxation is relatively weak due to the large internal friction force among the molecules and less molecule mobility. As the temperature increases, polymer enters the elastic region and will gain increased molecule mobility, this is accompanied by the increase in stress relaxation. When the polymer becomes more liquid state at even higher temperature, the material will become highly viscous and can loss elasticity.

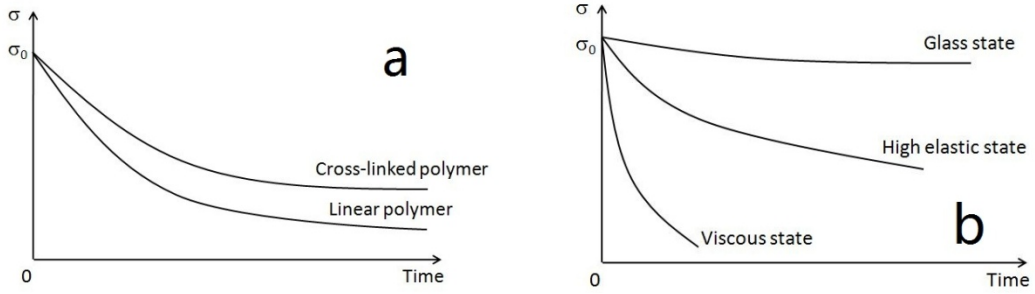

Figure 2.10 Stress relaxation (a) with different polymers, (b) with different states

2.2.3 Hydrogenated Nitrile Butadiene Rubber (HNBR)

2.2.3.1 Introduction to Elastomer

Elastomers are usually defined as polymers with significant viscoelasticity. Elastomers generally have a low Young's modulus and a high failure strain compared with other polymeric materials[40]. Most of the elastomers are thermoset polymers in which the long pre-polymer chains crosslink during curing. Such elastomer molecular structures often contain significant portion of space among the polymer chains and their elasticity is derived from the ability of the long chains to reconfigure themselves to distribute the externally applied stress. On the other hand, the covalent cross-linkages between molecular chains ensure that the elastomers to return to its original configuration when the stress is removed. Elastomers normally exist in the state above their glass transition temperature. When the temperature is below its glass transition temperature, elastomer molecules will have less mobility and elasticity is lower. Based on their unique mechanical properties, elastomers are extensively used in seals, adhesives and molded flexible parts.

2.2.3.2 Background Information on Nitrile Rubber (NBR) and Hydrogenated Nitrile Rubber (HNBR)

Nitrile rubber (NBR) was first commercialized in Germany, in1937, under the trade name of Buna N. It is a copolymer of butadiene and acrylonitrile, and since has been extensively used as oil-resistant rubber[41, 42]. The acrylonitrile content in NBR determines the ultimate properties of the elastomer.

The heat resistance of NBR is directly related to the acrylonitrile content (ACN) in the elastomer. In NBR the presence of double bond in the polymer backbone makes it susceptible to heat, ozone, and light. In comparison, hand the more recently developed fluoroelastomers can have much better mechanical and chemical performances, but their cost is much higher. So there are many efforts in improving NBR properties, and HNBR is one typed of modified NBR that has been developed to bridge the price- performance gap.

2.2.3.3 Manufacturing Process of NBR and HNBR

Schematics of a NBR manufacturing facility is shown in Fig. 2.11

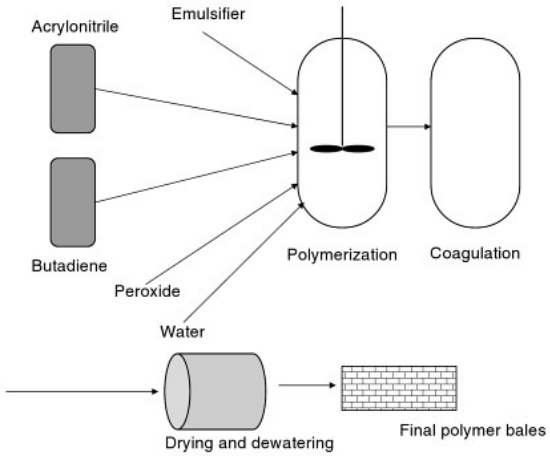

Figure 2.11 Schematic of NBR Polymerization Process

Chemical reaction to form NBR is shown in Fig 2.12. During the process, butadiene and acrylonitrile monomers are introduced in the presence of emulizer and peroxides to form polymer[43, 44]. The polymer will then go through a hydrogenation process as shown in Fig 2.13. It should be noted that there are two different types of butadiene units existed in the original NBR polymer, they are the cis-1,4-unit and the trans-1,4-unit. After hydrogenation, some of the two butadiene units will become saturated and become the

same. But because the hydrogenation process favors the 'vinyl' type units more than the butadiene units, thus there will always be remained unsaturated butadiene units in NBR.

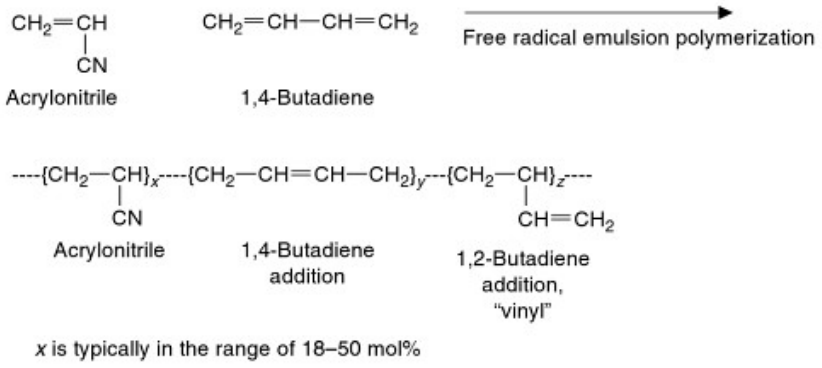

Figure 2.12 NBR Polymerization

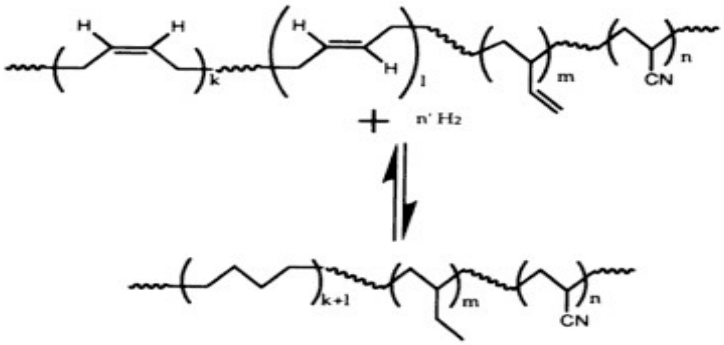

Figure 2.13 Hydrogenation of NBR

HNBR can be obtained through controlled hydrogenation reaction of NBR, Fig 2.14 shows the schematic of a HNBR manufacturing process[45].

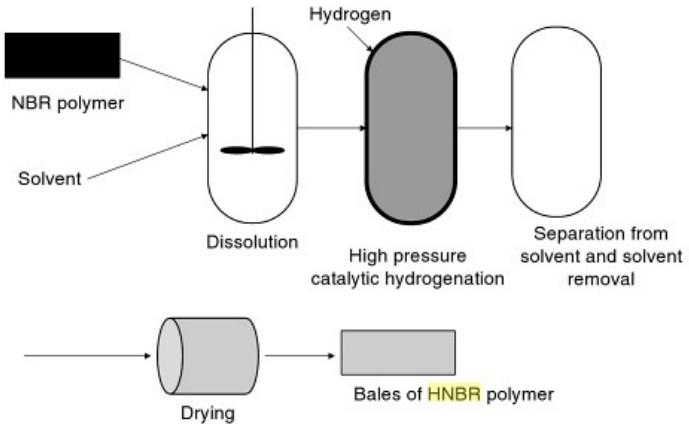

Figure 2.14 Schematic of NBR Hydrogenation Process

2.2.3.4 Catalysts used in NBR Hydrogenation Process

Catalysts are needed to introduce the hydrogenation reaction in NBR to form HNBR. Supported Palladium is currently the most widely used catalyst for hydrogenation of conjugated diene polymers containing nitrile group[46, 47]. Palladium has a much lower cost comparing to the Rhodium-based catalysts, but with poor mechanical property. So an active porous support or alloying are needed to develop the Pd based catalyst. Palladium and aluminum, palladium on carbon and palladium supported on silica are the commonly used NBR hydrogenation catalysts. Other reported catalysts include, silica-supported palladium and lithium acetate promoter, palladium on calcium carbonate, palladium supported on titanium dioxide, polymer-supported catalyst

Most of the NBR hydrogenations reactions were carried out under a 5.0 MPa hydrogen pressure, at 50℃ temperature, and for 4-6 h. Acetone is the commonly used solvent to dissolve HNBR while tetrahydrofuran (THAF) and isobutyl-methyl ketone are also used. Not many detailed fundamental study on the heterogeneous catalytic

hydrogenation reaction of nitrile rubber can be found in literature that can provide an insight into the reaction. Most of the available information is from patents.

In comparison, the principle of homogeneous catalytic hydrogenation is better understood. The process takes place through the activation of molecular hydrogen by the transition metal complex in solution and subsequent hydrogen transfer to the unsaturated NBR. The most important advantage offered by homogeneous catalysts is their selectivity as compared with heterogeneous reactions.

The NBR hydrogenation process for most of the catalyst systems follows the same route. At first the polymer is dissolved in a suitable organic solvent. The solution is purged with hydrogen and then appropriate amount of the catalyst is added. The mixture is subjected to the desired temperature and hydrogen pressure. After the completion of the reaction, the mixture is cooled and the polymer is precipitated out and finally dried. The reaction can be controlled up to the desire level of hydrogenation by proper combinations of the reaction pressure, temperature, time, and catalyst concentration[48-51].

2.2.3.5 Curing process

Sulfur and peroxides are the most used curing agents for HNBR[52]. Sulfur is more cost effective, but because HNBR is a highly saturated polymer, peroxides are more efficient.

Vulcameter is used to determine parameters of curing process, includes pressure, temperature and curing temperature. The curing process mainly consists of two stages, press-curing and oven post-curing (usually with 2h). Additives can be added into polymer during these curing processes to obtain desired amorphous structural.

2.3 HNBR Applications

Since HNBR is a highly saturated nitrile rubber, it delivers resistance to oil, gas and steam that is superior to standard nitrile butadiene rubber and other polymers. Depend on filler selection and loading, HNBR compounds can have tensile strengths as high as 20-31 MPa when measured at 23□C depend on the degree of hydrogenation. With compounding techniques, HNBR can be used over a broad temperature range, -40□C to 165□C, with minimal degradation over long periods of time. Compare with other polymer composites, HNBR elastomers not only have poor electrical and flame resistance, but also possess excellent resistance to common automotive fluids, such as engine oil, coolant, fuel, etc. The unique properties attributed to HNBR have resulted in side adoption in industrial, including automotive seals, hoses and synchronous timing belts. Also HNBR has been widely employed in industrial seals for oil field exploration and processing, as well as rolls for steel and paper mills.

2.4 Polymer based Composites

2.4.1 History of polymer based composites[53, 54]

The history of developing polymer based composites can be traced back to the 1940s, directly driven by the world war Ⅱ. Polymer composites are development to meet the demands of high-strength, light-weight materials. When the improvements on traditional metal based components become limited, scientists turned to the newly-developed polymer industry. During that period of time, many new and light-weight polymers were synthesized. In the meanwhile, glass fibers were also discovered during the same period

of time, they have shown extremely high strength. So researchers were also interested in how to use these potentially high-strength materials to solve the problems posed by the military's demands. By immersing glass fibers in a matrix of a lightweight, low-strength material, a stronger material could be obtained because the fibers stop the propagation of the cracks in the matrix. This contributed to the beginning of the reinforced plastics industry: GFRP (glass fiber reinforced polymer). GFRP technology spread rapidly in the 1950s. For example, fiberglass-polyester was used to produce the sleek body of the corvette sports car. In the 1960s, space and aircraft demands had prompted the quest for new high modulus fibers. Graphite fibers were produced which took the lead in reinforced composites due to its superior processing capabilities and its lower cost. With the development in this field, both academic and industrial researchers started to extend the composite paradigm to smaller and smaller scales, polymer based composites are more likely to be considered as nanocomposites these days and widely used in aerospace, transportation, civil, automotive and electronics industries.

2.4.2 Advantages of Polymer Based Composite

As mentioned before, by combining different material together, polymer composites possess not only physical properties of each component, but also have following improved properties that are not possessed by pure matrix materials[55, 56].

1. High strength to weight ratio and high modulus to density ratio. Polymer material normally has low intrinsic strength and modulus, by adding high strength filler inside, composite can achieve a higher strength and higher modulus.
2. High fatigue resistance. Metals are prone to failures caused by fatigue. But for

polymer composites, by adding fillers inside, fatigue resistance is higher and more time for material to response to fracture.

3. Good cushioning ability. The nature vibration frequency of a structure is dominated by its structure configuration as well as the square root of the strength weight ratio. Due to high strength weight ratio of polymer composites, the natural vibration frequency of composite can be relatively high.
4. Design and manufacture flexibility. Different properties can be obtained by adjusting the composite components ratio. Also changing the filler orientation, layer sequences can also effectively alter the properties of composites.

2.4.3 Current compounding and manufacturing techniques

Fillers in composites are especially useful in industrial applications, hence products in mass production is demanded urgently nowadays. Common techniques have been employed, such as sheet molding compound (SMC), direct-compounded long-fiber thermoplastic (D-LFT) and injection molding (IM).

Sheet Molding Compound (SMC)

Sheet Molding Compound (SMC) is a compression molding compound often used for larger parts where higher mechanical strength is needed. Thermoset Sheet Molding Compound is a mixture of polymer resin, inert fillers, fiber reinforcement, catalysts, pigments and stabilizers. As shown in Fig 2.15, manufacture of sheet molding compounds is a continuous in-line process. The material is sheathed both top and bottom with a plastic film to prevent adhesion. The paste is spread uniformly onto the bottom film. Chopped glass fibers are randomly deposited onto the paste. The top film is

introduced and the sandwich is rolled into a pre-determined thickness. Due to its low labor requirements, this technique is widely used in automotive composites industry.

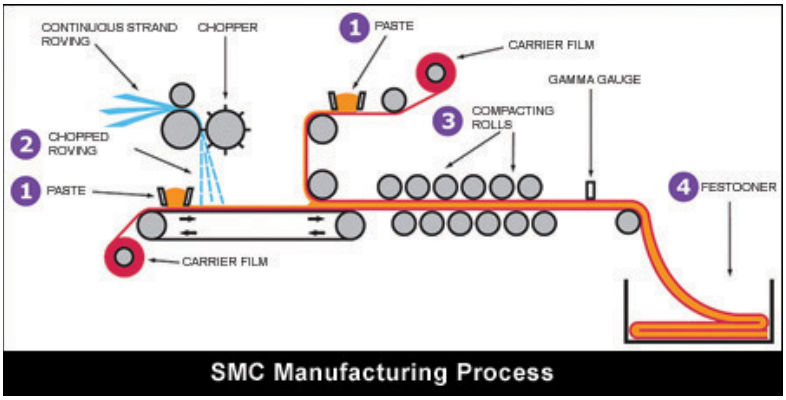

Figure 2.15 Schematic drawing of SMC manufacturing process

Direct-Compounded Long-Fiber Thermoplastic (D-LFT)

Long fiber thermoplastic molding is a newer technology where thermoplastic material is directly compounded with long glass fibers and then molded in one operation as shown in Fig 2.16. The advantage of D-LFT is the ability to control the length of the fiber being mixed into the thermoplastic pellets via an extruder.

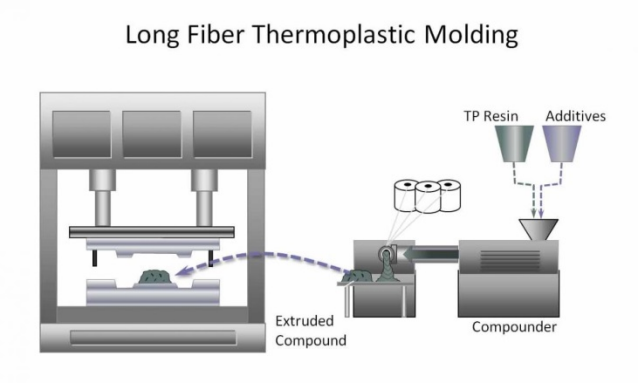

Figure 2.16 Schematic drawing of D-LFT

Injection Molding

Injection molding is widely used in manufacturing industry for its simple process steps. By feeding a host of materials, including thermoplastic and thermosetting polymers, fillers and additives, into a heated barrel, mixed, and forced into a mold cavity for cooling down as shown in Fig 2.17. The advantage for this technique is that large, complex, 3-dimensional parts can be created with appropriate preform at the compensation of high cost.

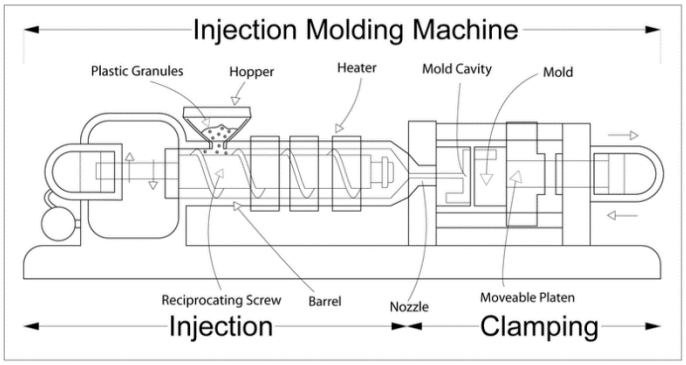

Figure 2.17 Schematic of injection molding machine

Chapter 3 Research Objectives and Scope of Work

HNBR is the current the industry workhorse for developing sealing, connection and protection products. Their high temperature stability and chemical resistance (especially to H_2S) make them the elastomer of choice for many downhole applications. Yet HNBR is more prone to extrusion than standard nitrile rubber, so it is of great interest and importance to modify and improve its mechanical properties. In this study, we first explore the synthesis of carbon nanofiber filled HNBR and evaluated the reinforcement of this one-dimensional nanomaterial. We also studied the fabrication and properties of using hybrid-reinforcement, where the CNF is added with conventional carbon black and silica fillers. The use of fillers with different morphology, size and chemistry allow us to tune HNBR mechanical properties without significant cost increase. The CNF and hybrid reinforced HNBR nanocomposites can have extensive application potentials in seal development. In order to accomplish the research and development objectives, the specific scope of work are discussed in following sections:

1) Explore solution based composite synthesis procedures
2) CNF surface functionalization
3) Investigation of the morphology of filler reinforced composite
4) Determine the stress-strain behaviors of composite samples with different amounts of fillers
5) Compare the complex modulus for different composite samples
6) Evaluate the thermal stability of different composite samples

Chapter 4 Experimental Setup, Methods and Sample Fabrication

4.1 Experimental Setup and Methods

4.1.1 Instron Tensile Tester and Accessories

In order to investigate the stress-strain relation, we are employing Instron tensile tester Model No. 5944 with a long travel extensometer. Two pneumatic grips are used to fix the dumbbell sample with one end to the bottom of the tester while the other attached to a moveable 1 kN load cell. The advantage of the pneumatic grips is that it applies large force to the heads of the samples which reduce the sample slippage effectively. Schematic graph of the tensile tester with sample is shown in Fig 4.1. While moving the cross-head with a speed of 20 in/min, applied force is measured by the load cell and recorded by the computer and total sample deformation data is recorded by extensometer as for engineering stress and strain calculation.

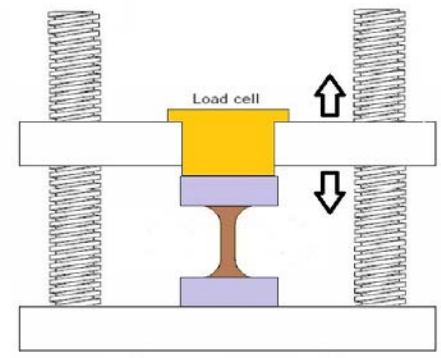

Figure 4.1 Schematic of tensile tester

This experiment is performed under the guidance of ASTM standard D 412 with confined shape and dimensions as shown in Fig 4.2.

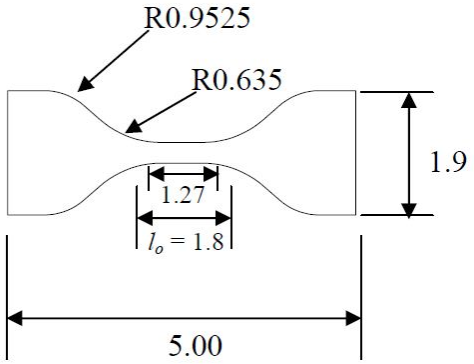

Figure 4.2 Dimensions of dog-bone shaped tensile sample

The thickness of the sample before tensile test is measured by a micrometer for stress calculation. From the measured load and deformation data, sample modulus can be calculated use following equation:

$$E \equiv \frac{tensile\ stress}{tensile\ strain} = \frac{\sigma}{\varepsilon} = \frac{F/A_0}{\Delta L/L_0} = \frac{F \times L_0}{A_0 \times \Delta L} \quad . \qquad (4.1)$$

4.1.2 Dynamic Mechanical Analysis

Dynamic mechanical analysis (DMA) is used to characterize the dynamic response of sample. It is most useful for studying the viscoelastic behavior of polymers. During DMA measurement, an oscillating force to the sample and the material's response to the dynamic loading. A representative DMA setup and the applied force and deformation characteristic behavior are shown in Fig 4.3. In a typical measurement, when a sinusoidal stress is applied to sample, a sinusoidal strain will be generated. Materials viscoelasticity will present through a phase difference between the stress and strain functions. By measuring both the amplitude of the two curves and the lag between the stress and strain sine waves, a complex modulus can be determined. The real part of the complex is termed as the storage modulus and reflects the elasticity of the material, the imaginary

part of the complex defines the loss modulus, which reflects the viscosity and the damping of the material. Polymer viscoelasticity strongly depends on temperature, so is the material complex modulus. So DMA can be used to determine the temperature dependent polymer transition. It can be used to determine the glass transition of polymer as well as other transformation of molecules due to temperature variation.

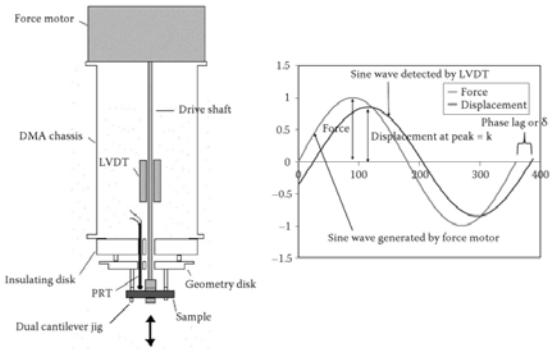

Figure 4.3 Schematic shows how DMA works

DMA can be operated in several different modes. These measurements modes have different fixtures and designed for deferent types of samples. Measurement purpose can also be different. The common DMA measurement modes include the single cantilever bending, dual cantilever bending, 3-point bending, tension film fixture, tension fiber fixture, compression fixture and shear fixture. In the current research, the tension film fixture is employed with the typical testing sample dimension of :30mm (L) × 6.43mm (W) × 2mm (T). The typical measurement temperature range is from -50 ˚C to 150 ˚C.

4.1.3 Differential Scanning Calorimeter

Differential scanning calorimeter (DSC) is a thermoanalytic instrument which measures the heat adoption/release difference between a sample and a reference with the changing temperature. The sample and the reference are maintained in the same condition

and the thermal properties of the reference pre-determined. Most commonly, the temperature in DSC is designed to increase linearly as a function of time. By recording the heat flow into/out of the sample, heat capacity change of material versus temperature can be recorded, and the phase transition can be identified from such a curve. The basic principle underlying this technique is that when the sample undergoes a physical transformation, the heat capacity of the sample will deviate from a linear change.

4.1.4 Thermogravimetric analyzer

Thermal-gravimetric analysis (TGA) is a form of thermal analysis that measures the material change in physical and chemical properties with increasing temperature. It measures the material mass change when varying temperature to provide information on selected material characteristics that relates to mass. In our stay, TGA is used to evaluate the thermal stability of our sample. Upon heating, different components will have their characteristic reactions at certain temperatures. Fig 4.4 shows the TGA Q500 used in this study. In the TGA measurement, a sample with known mass is first put appropriate on a acetone-cleansed platinum plate and placed in the cylindrical oven. Weight of the sample is continuously record when the temperature ramp from room temperature to 550 °C. Weight loss data are then to be analyzed.

Figure 4.4 Picture of the thermal gravimetric analyzer

4.2 Sample fabrication

4.2.1 Materials

Major component: Hydrogenated Nitrile Butadiene Rubber (HNBR) as rubber matrix, Carbon nanofiber (CNF) as prime filler with carbon black and silica. **Zinc oxide**, is an inorganic compound with the formula ZnO, has high refractive index, high thermal conductivity, binding, antibacterial and UV-protection properties. It is widely used in the vulcanization of rubber. **Stearic acid**, is a saturated fatty acid with an 18-carbon chain with the chemical formula $CH_3(CH_2)_{16}CO_2H$. It is used accompany with zinc oxide as vulcanization agent. **HVA-2** is yellow powder with chemical formula $C_{14}H_8N_2O_4$. Being a kind of multifunctional rubber vulcanizing agent, HVA-2 is used as vulcanizing agent and cocuring agent for peroxide system in rubber process. It can effectively improve correlation performance and heat resistance, thus preventing gross rubber from scorching during process. **VC-60 VUL-CUP** is peroxide curative. It forms crosslinks in the nitrile

rubber which increases the thermal stability. The stronger crosslinks formed by peroxide vulcanization provide superior heat aging and compression set.

All components are listed in table 4.1.

Solvent acetone is applied for dissolving HNBR and fillers in order to get a uniform solution.

Table 4.1 Components of Composite

Recipe in phr	VGUH-00	VGUH-01	VGUH-02	VGUH-03	VGUH-55	VGUH-04	VGUH-22	VGUH-23	VGUH-24	VGUH-25	VGUH-26	VGUH-27
Description	phr	phr	phr	phr	phr	phr	phr	phr	phr	phr	phr	phr
ZETPOL	100	100	100	100	100	100	100	100	100	100	100	100
CNF	0	40	40	40	40	40	40	40	40	30	20	10
ZnO911C-85/NBR/S	5	5	5	5	5	5	5	5	5	5	5	5
STEARIC ACID ACTIVATOR	0.5	0.5	0.5	0.5	0.5	0.5	0.5	0.5	0.5	0.5	0.5	0.5
HVA-2/ VANAXMBM	2.5	2.5	2.5	2.5	2.5	2.5	2.5	2.5	2.5	2.5	2.5	2.5
CARPLEX 1120	0	0	0	3	5	8	10	15	25	25	25	25
N326 CARBON BLACK	0	0	1	3	5	8	10	15	25	25	25	25
VC-60 VULCUP	5	5	5	5	5	5	5	5	5	5	5	5
Total	113	153	154	159	163	169	173	183	203	193	183	173
Recipe in gm	VGUH-00	VGUH-01	VGUH-02	VGUH-03	VGUH-55	VGUH-04	VGUH-22	VGUH-23	VGUH-24	VGUH-25	VGUH-26	VGUH-27
Description	gm	gm	gm	gm	gm	gm	gm	gm	gm	gm	gm	gm
ZETPOL	300	300	300	300	300	300	300	300	300	300	300	300
CNF	0	120	120	120	120	120	120	120	120	90	60	30
ZnO911C-85/NBR/S	15	15	15	15	15	15	15	15	15	15	15	15
STEARIC ACID ACTIVATOR	1.5	1.5	1.5	1.5	1.5	1.5	1.5	1.5	1.5	1.5	1.5	1.5
HVA-2/ VANAXMBM	7.5	7.5	7.5	7.5	7.5	7.5	7.5	7.5	7.5	7.5	7.5	7.5
CARPLEX 1120	0	0	0	9	15	24	30	45	75	75	75	75
N326 CARBON BLACK	0	0	3	9	15	24	30	45	75	75	75	75
VC-60 VULCUP	15	15	15	15	15	15	15	15	15	15	15	15
Total	339	459	462	477	489	507	519	549	609	579	549	519

4.2.2 Preparation of composition

In this study, a solution based mixing approach was adapted to improve the filler dispersion. In a typical sample fabrication process, carbon nanofibers, carbon black and silica were placed in acetone with desired ratio. The suspension was then put into ultrasonicator to break up the agglomeration of fillers. In the meanwhile, bulk HNBR was roll-pressed into sheet form and then cut into pieces. The weighed HNBR pieces were then added into to filler suspension, and mixed mechanically for 2 hours with an electric

stirrer. Towards the end of mechanical mixing, 5phr ZnO911C-85, 0.5phr stearic acid activator and 2.5phr HVA-2 were added into the mixture and mix for another 3 hours with design for uniform blend as shown in Fig4.5. Phr is employed in rubber industry as a unit meaning that how much weight in 100 gram rubber matrix. Subsequently, distill acetone from solution in water bath as shown in Fig 4.6. Mix the desiccated master batch with VC-60 VULCUP on two roll mill for 10 min. Obtain the rubber composites after curing the master batch in hot press for 20 min at 320°F. Cut the composite sheet with specific die under standard ASTM D412.

Figure 4.5 Mechanical mixing process

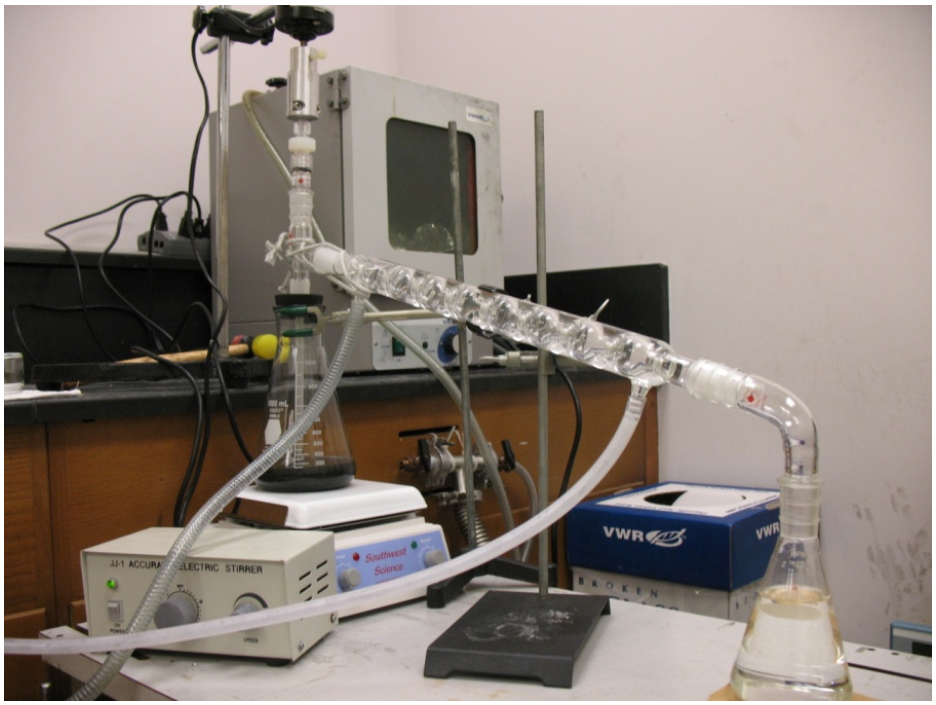

Figure 4.6 Distillation equipment

Chapter 5 Experimental Results and Discussion

Here we will discuss the observations in our nano-reinforced HNBR composites. We will focus on the microstructure, mechanical and thermal analysis of the samples.

5.1 Sample Morphology Study

5.1.1 The Morphology of conventional fillers

Carbon black and silica have been used in the rubber and plastic r industry for a long time for strength, modulus and erosion resistance enhancement. Also their price and availability make large scale industrial application possible. In our study, the conventional carbon black and silica are used as in the reference HNBR samples and also as the components to form hybrid reinforcement with CNFs.

As any other composite materials, filler dispersion and distribution control and uniformity are rudimentary requirements for polymer composite production and application. In this study, a liquid phase mixing method was developed.

First we look at the size and morphology of the conventional carbon black and silica used in this study. Powder of the raw carbon black and silica was placed in separate containers filled with acetone. The containers were then placed under ultrasonication for 30 min. A drop of suspension was taken from each solution and dripped onto a polished copper substrate for SEM examination after acetone evaporation. From the microscopic pictures with same magnifications as shown in Fig 5.1, we can see that carbon black and silica are nanoscale particles. The carbon black has an average diameter around 40 nm and the silica has average size found 100nm. Carbon black has

more defined spherical shape and smaller size distribution than the silica parties.

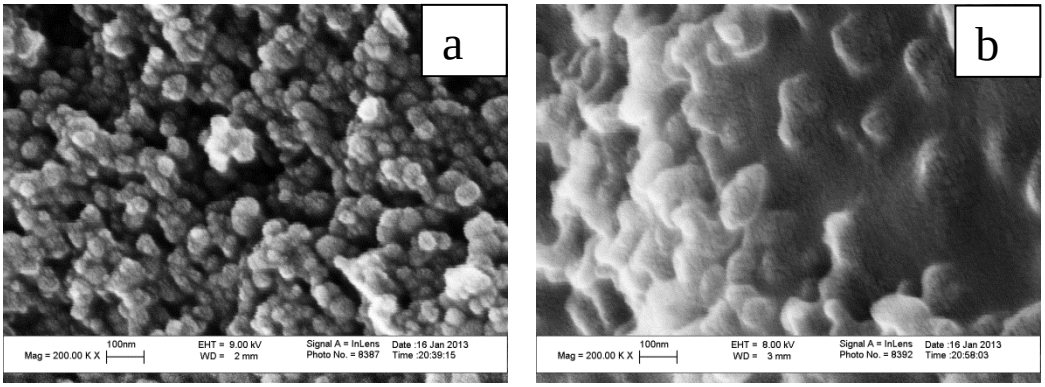

Figure 5.1 SEM micrographs of Carbon black (a) and silica (b)

5.1.2 The Morphology of Nanocomposites

Cross-section morphological micrographs of the composite samples were taken after sample fracturing using SEM. Fig 5.2 shows the pictures of a HNBR fractured surface at two different magnifications of composite with 21.6phr CNFs, 4.7phr carbon black and 4.7phr silica. Pulled out carbon nanofibers with average diameter of around 100nm and length on the order of tens of microns can be clearly identified. This observation also indicates that during normal tensile pull-out tests, the CNF-HNBR interface fails before the CNF, this is not surprising considered its high strength. It also implies that by modifying the CNF surface and improving interfacial bonding, the nanocomposite mechanical performances can be further improved. In these two pictures, we can observe also observe the existence of large number of embedded particles, it is very difficult to differentiate between these carbon black and silica particles in the HNBR matrix.

Fig 5.3 compares the cross-section morphology of two HNBR composite samples with different filler concentrations. The fractured composite surface show quite different morphology, where the lower carbon black/silica filled surface has a more homogenous

structure. Carbon and silica has the tendency to agglomerate and they form a layered structure. Due to their poor electron conductance, they appear in greater brightness in the SEM. So with high carbon black and silica concentration, the sample fracture surfaces show white layered structure. How this affects the composites' mechanical properties will be illustrated in the next part.

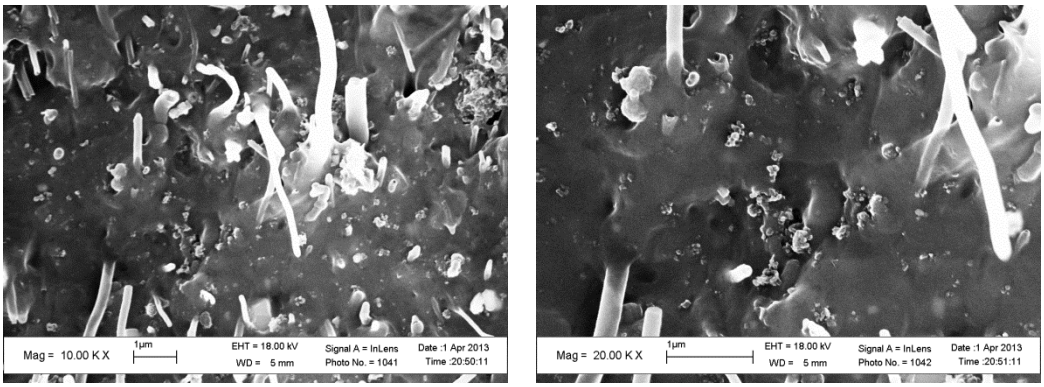

Figure 5.2 SEM micrographs of hybrid filler composites

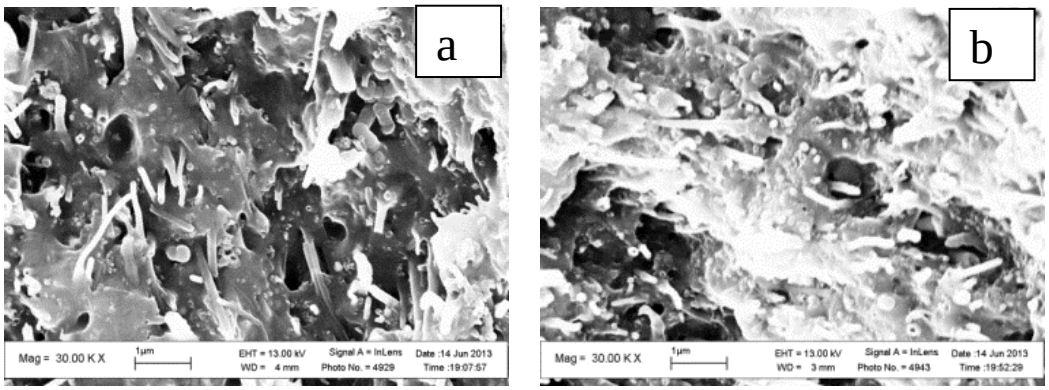

Figure 5.3 (a) 5phr carbon black and 5phr silica with 40phr CNF in HNBR; (b) 25phr carbon black and 25phr silica with 40phr CNF in HNBR

5.2 Mechanical properties

5.2.1 HNBR with carbon black and silica

First we look at the reinforce effect of conventional carbon black and silica on HNBR. Since the stress-strain train response of the HNBR and composites is non-linear,

we use the secant modulus to describe the elastic strength of our samples. The secant modulus is the slope of line connecting the origin and the stress at certain strain levels. Figure 5.4a summarized such moduli data calculated for four samples with different carbon black/ silica concentrations at different strain levels. It is obvious that adding the conventional fillers to HNBR can effectively improve polymer modulus. The modulus enhancement effects increase with filler addition. The results are consistent with previous work[57]. Also even at a 40phr level, there is no significant deterioration in sample ductility. From the cross-sectional SEM image of Fig 5.4b, we can see the fillers mostly have spherical shape with very uniform distribution. Agglomeration can is can be observed, but their sizes are below 1 micron.

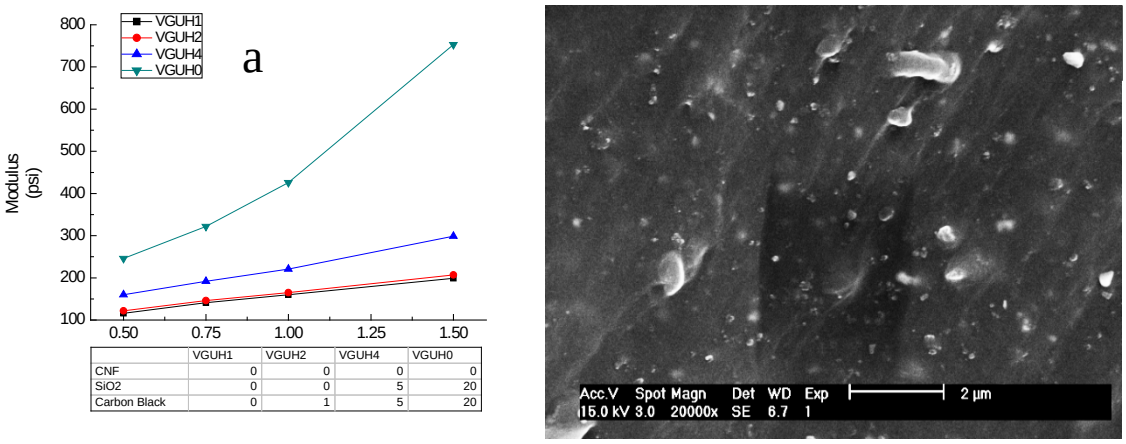

	VGUH1	VGUH2	VGUH4	VGUH0
CNF	0	0	0	0
SiO2	0	0	5	20
Carbon Black	0	1	5	20

Figure 5.4 (a) Stress-strain curve of HNBR with carbon black and silica; (b) Distribution of carbon black and silica in HNBR

5.2.2 HNBR/CNF composition

In this experiment, we study the reinforce effect of CNF, no carbon black/silica were added. As shown in Fig 5.5(a), same as the previous experiments, the pristine HNBR possesses low tensile stress and tensile strength. Not surprisingly, CNF enhancement

effect also increases with concentration. Normalized by added CNF concentration, the biggest increase in modulus enhancement happens when the added CNF concentration is in between 10-20phr.

In this study we also evaluated the effects of acid treatment on mechanical properties of CNF-HNBR. A comparison between sample VGUH5 and VGUH6 shows that for the same CNF concentration of 10phr, great enhancement in sample modulus at 75% strain can be achieved after CNF surface acid treatment. Morphology study performed on fractured composite samples as Fig 5.5(b) shows that the CNF have quite uniform distribution in the HNBR. From previous research[58], we found that acid treatment can remove catalysts in the raw CNF and break up CNF entanglement. It is also believed that the treatment can introduce functional –COOH and $–NH_2$ groups to the CNF surface. Due to these effects, acid treated CNFs will have better dispersion and form better bonds with the matrix. However, the acid treated samples normally will have less ductility, this could be due to the fact that, acid attacks CNF surface and reduced CNF length and decreases the effectiveness in reducing fracture propagation.

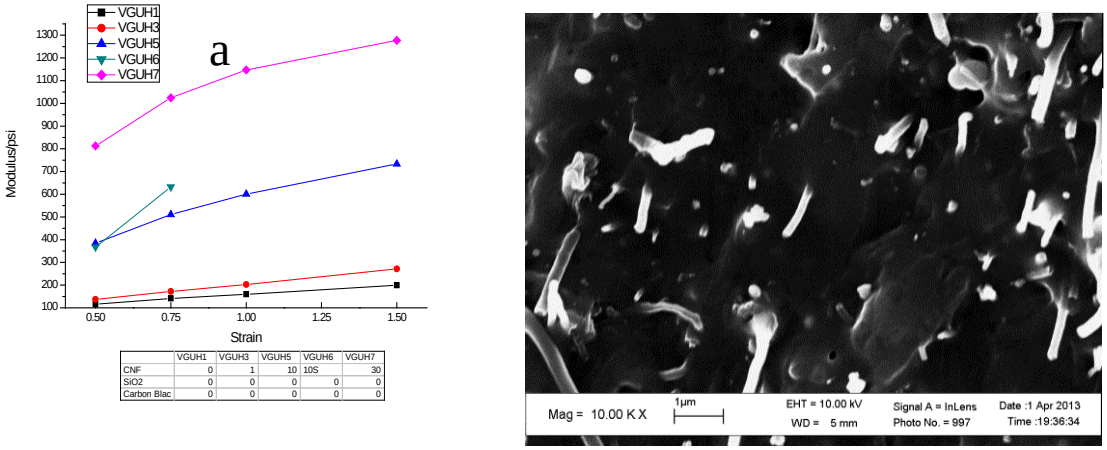

Figure 5.5 (a) Stress-strain curve of CNF composites; (b) Morphology of CNF in HNBR

5.2.3 HNBR Composites with Hybrid Reinforcement

Conventional HNBR seals have 40phr or higher combined carbon black and silica concentration. We have shown that with the same concentration, CNF fillers can provide better enhancement effect than conventional carbon black and silica, the cost increase of using CNF may not be well justified for some of the HNBR applications. So we want to explore the development of hybrid enhanced composites, the hypothesis is due to the size and shape differences between the two types of fillers, there will be enhanced effects beyond the simple combination effects from the two fillers.

In the first serial of experiments, we fix the carbon black and silica concentration, and increase the CNF concentration from 10 to 40phr. Fig5.6a shows the stress-strain curves from four of such samples. It clearly shows that the increased CNF concentration can further increase to the mechanical strength of HNBR reinforced by carbon black and silica. Fig 5.6b shows the modulus enhancement at 50% strain for these hybrid composites. With only carbon black and silica addition the HNBR modulus is about 200psi, the 10 phr addition of CNF increase the sample modulus to 1000 psi Then there is an almost linear dependence between the sample modulus and CNF concentration between 10 to 40 phr CNF and achieves 2000Psi at 40phr. This value is about 20 time of the pure HNBR modulus.

Accompany of significant sample modulus enhancement is the decrease of ductility. Pure HNBR can sustain a 300% of strain before fracture. The sample ductility reduces to about 80% for our samples with maximum amount of fillers. Apparently, the decrease of polymer percentage, increase in the filler-polymer interface and more surface debonding are among the main reasons of this ductility reduction. Adding fillers to the HNBR has

small effect on the tensile strength of the HNBR. Only a small increase in tensile strength has been observed with increasing filler concentration.

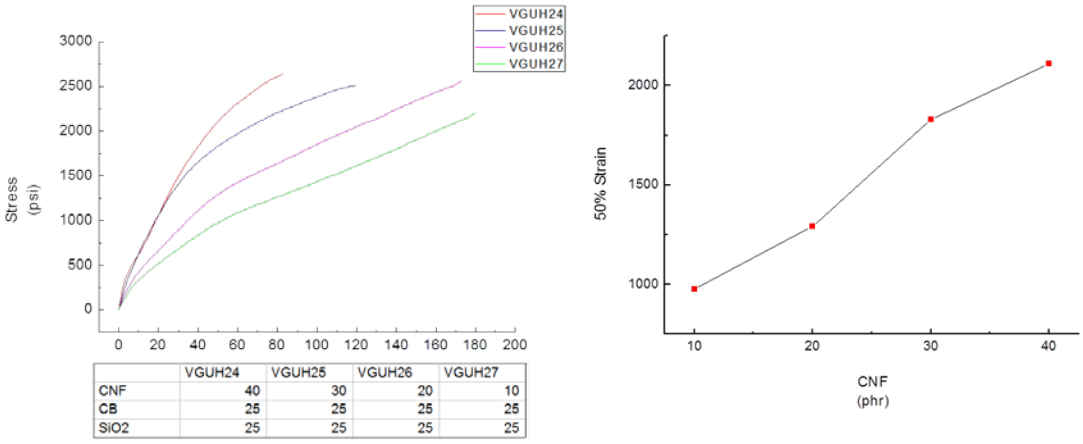

	VGUH24	VGUH25	VGUH26	VGUH27
CNF	40	30	20	10
CB	25	25	25	25
SiO2	25	25	25	25

Figure 5.6 (a)Stress-strain curve of different amount conventional fillers; (b)Moduli trend with 50% strain.

In the hybrid reinforcement, HNBR mechanical properties are affected by both carbon black/silica and CNF concentrations. So in this study, we also investigate carbon black and silica impact the modulus of hybrid composites. In this part of study, CNF concentration in the sample is fixed at 40phr and the carbon black/silica concentration changes from 0 to 50phr. Fig5.7 shows stress and strain curve of samples with 8phr conventional filler concentrations. It shows that addition of conventional filler can also enhance the already improved HNBR modulus. Also the modulus enhancement comes at the cost of lower sample ductility. When plot out the modulus versus conventional filler concentration we see a non-monotonic correlation between the two. Instead having a continuous increase, the sample modulus has a fast initial increase with carbon black/silica addition, and reaches its maximum value at about 8phr carbon black and 8phr silica. Sample modulus then has a sharp drop to 20phr carbon black/silica addition, and followed by as slow increase at higher filler concentrations. We believe the filler

distribution in HNBR plays the most important role in determining these mechanical behaviors of the composite. The best reinforcement effects happen with uniform filler distribution. As shown in earlier study, carbon black and silica tend to aggregate at high ratio. The addition of CNFs will significantly affect the conventional filler distribution since they tend to form interconnect structures. These structures will significantly increase local viscosity during mixing and further affect filler distribution at high carbon black/silica concentrations. We believe at the small conventional filler concentration, uniform distribution can be achieved with less agglomeration. Once the amount of fillers is larger than 10phr, severe particle agglomeration will happen and it will lead to less polymer distribution uniformity and create weak bonding regions. From SEM images shown in Fig5.8b, we can find layer structure of carbon black and silica was formed due to the high degree agglomeration. At even higher ratio of carbon black and silica concentrations, slower modulus increases can be observed and we attribute to the increased interaction between fillers and rubber matrix, but the achievable modulus is still lower than the highest level achieved at 16phr combine carbon black/silica addition.

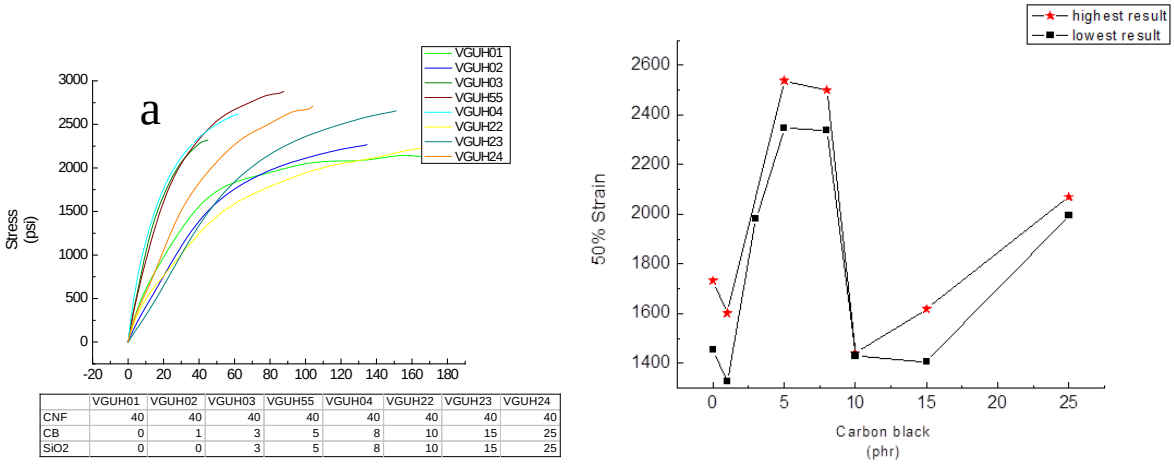

	VGUH01	VGUH02	VGUH03	VGUH55	VGUH04	VGUH22	VGUH23	VGUH24
CNF	40	40	40	40	40	40	40	40
CB	0	1	3	5	8	10	15	25
SiO2	0	0	3	5	8	10	15	25

Figure 5.7 (a) Stress-strain curve of hybrid fillers in HNBR; (b) Modulus trend in 50% strain

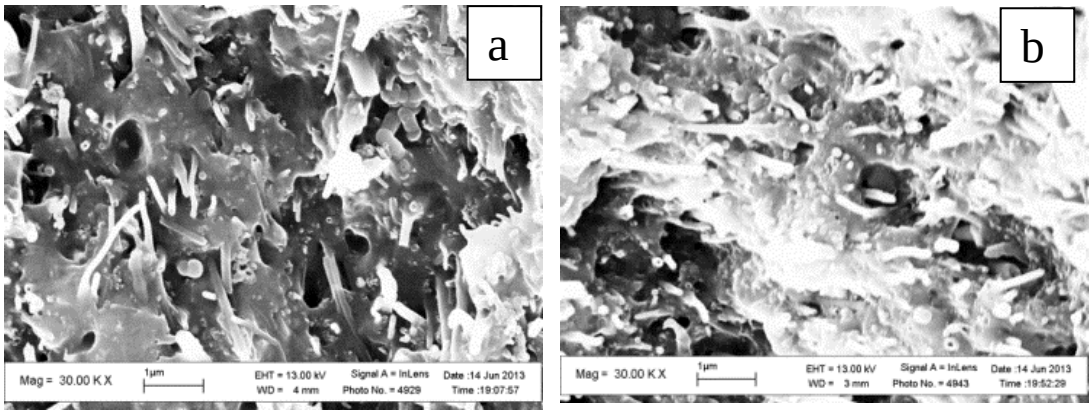

Figure 5.8 (a) 5phr carbon black and 5phr silica with 40phr CNF in HNBR; (b) 25phr carbon black and 25phr silica with 40phr CNF in HNBR

5.2.4 Dynamic Mechanical Properties of Hybrid Composites

Dynamic mechanical analysis is conducted in tension mode with temperature sweep from -50 ˚C to 150 ˚C. As shown in fig5.9, the one with 8phr carbon black and 8phr silica possesses the highest complex modulus which is consistent with tensile test result with the same reason that the fillers are blended uniformly inside rubber matrix that strong bound rubber interaction dominates.

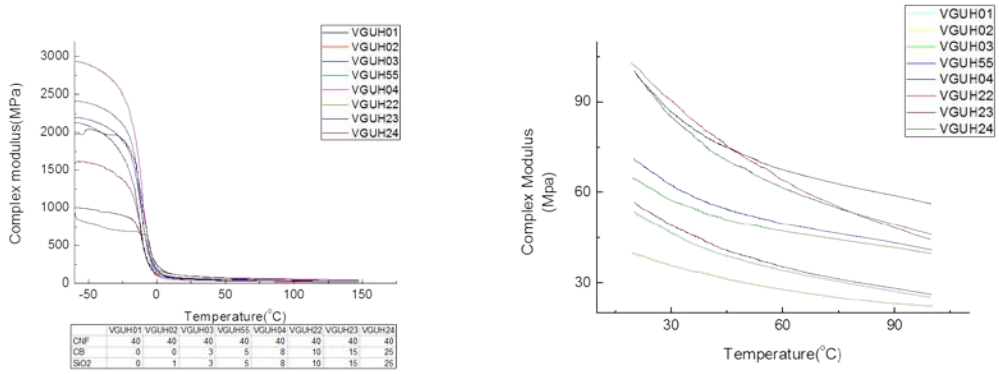

Figure 5.9 Effect of carbon black and silica on dynamic modulus with 40phr CNF

5.2.5 Differential scanning calorimeter

In DSC experiment, samples are measured in standard mode with temperature ramp 10 ˚C/min from -100 ˚C to 100 ˚C. By comparing pure HNBR with the one filled with 10phr CNF, glass transition temperature (Tg) for pure HNBR is -21.63 ˚C, Tg for filled-rubber is -23.09 ˚C shown in Fig5.10. No significant difference is discovered but only a few degree deviations. This indicates that carbon based nano-fillers cannot affect the chain structure of polymer but only mechanically adhere to polymer chain that generate bound rubber interaction.

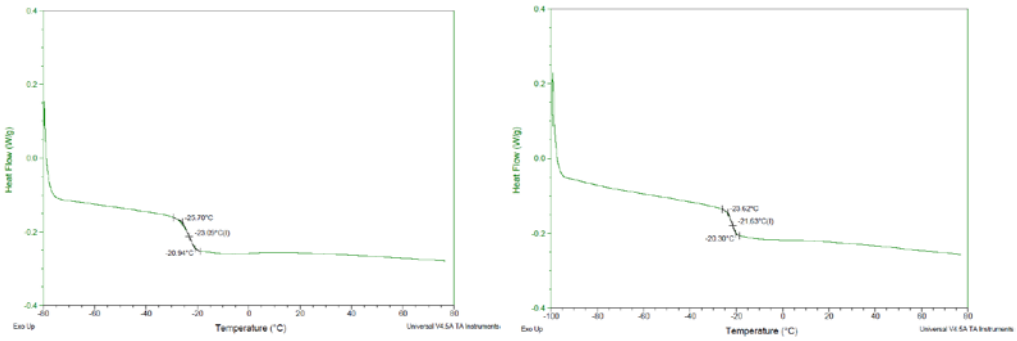

Figure 5.10 Differential scanning calorimetric result of non-filled rubber and filled composite

5.2.6 Thermal stability analysis

With the knowledge of fillers will not change the chain structure of polymer by DSC analysis, chemical properties also should not vary too much. Thermal gravimetric analysis is employed to ensure this argument. By comparing the weight loss under heat, thermal stability is examined as well as other chemical reaction. Fig 5.11 shows the weight loss with the temperature ranging from room temperature to 600 ˚C. Residue versus noncombustible components is also illustrated in Fig 5.12. All fillers like carbon

nanofibers, carbon black and silica possess good thermal stability during heating, HNBR matrix converts into ashes meanwhile. The linear result verifies the componential veracity of sample during manufacturing. Deviation may be caused by fillers' agglomeration in certain area.

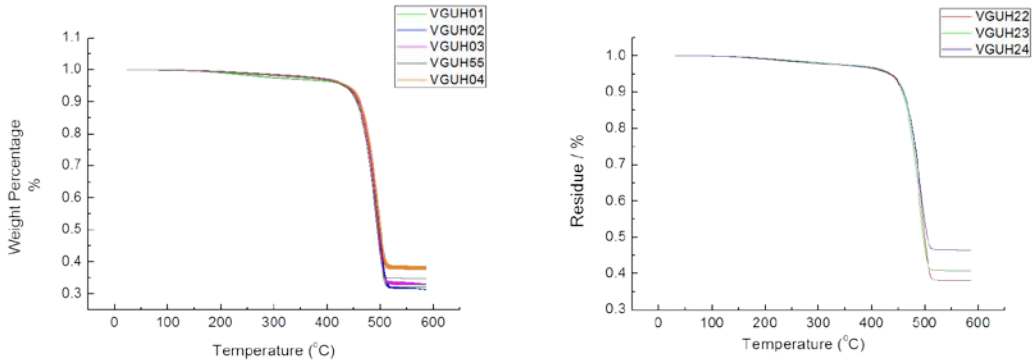

Figure 5.11 Weight loss versus temperature for all composites

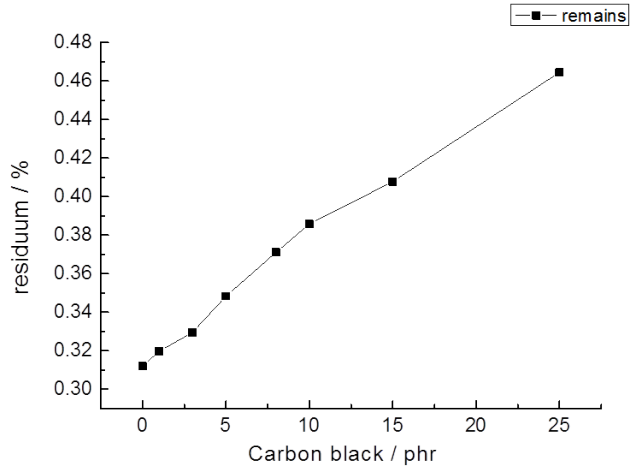

Figure 5.12 Residue versus carbon black ratio

Chapter 6 Conclusion

In present rubber industry, conventional fillers like carbon black and silica are widely used to increase the mechanical and thermal properties of certain rubber matrix. By adding carbon nanofibers(CNFs) with those conventional fillers, polymer nanocompoistes with more improved mechanical properties were produced. Polymer nanocomposites with carbon nanomaterial reinforcement have been extensively studied recently with expectations to utilize their superior physiochemical properties which are not possessed by conventional polymers. The most used polymer nanocomposite synthesis methods are direct mixing or *in situ* polymerization. The control of the nanomaterial dispersion and filler-matrix interfacial bonding remain as the most significant challenges for manipulating the microstructure and properties of the composite.

This study represents an attempt to develop a new filler-matrix system with improved control of nanofiller dispersion with higher reproducibility. Compare to pure HNBR, significant elastic modulus (E) enhancement has been observed after the introduction of CNF. Enhancement of 5 times (from 100 psi to 500 psi) and 20 times (from 100 psi to 2000 psi) have been observed in conventional fillers (20phr carbon black and 20phr silica) and hybrid fillers (40phr CNF, 25phr carbon black and 25phr silica) in HNBR, respectively. However, nanocomposites have a much decreased elastic deformation range due to the more surface debonding with the increasing fill-polymer interface. A sharp drop have been observed at 20phr carbon black/silica addition and followed by a slow increase at higher filler concentrations. As mentioned before, filler

distribution in HNBR plays a significant role in determining the mechanical behaviors of the composite. The best reinforcement effects happen with uniform filler distribution. Since carbon black and silica tend to aggregate at high ratio, the sharp drop is caused by filler agglomeration. With larger concentration, interconnect structures of the conventional fillers are formed which contribute to a slower modulus increase but with much more cost. Obviously this is not an optimized ratio for filler-rubber system.

Our approach of producing the CNF-elastomer nanocomposite is low cost, reproducible and easy to scale up. The high elastic modulus, large deformation tolerance and outstanding thermal stability of the nanocomposites make them the promising candidate as sealing materials.

Reference

1 BB Boonstra, "Role of Particulate Fillers in Elastomer Reinforcement: A Review," *Polymer,* 20 (1979), 691-704.

2 D Felhös, J Karger‐Kocsis, and D Xu, "Tribological Testing of Peroxide Cured Hnbr with Different Mwcnt and Silica Contents under Dry Sliding and Rolling Conditions against Steel," *Journal of Applied Polymer Science,* 108 (2008), 2840-51.

3 N Rattanasom, T Saowapark, and C Deeprasertkul, "Reinforcement of Natural Rubber with Silica/Carbon Black Hybrid Filler," *Polymer Testing,* 26 (2007), 369-77.

4 D Xu, J Karger-Kocsis, and AK Schlarb, "Friction and Wear of Hnbr with Different Fillers under Dry Rolling and Sliding Conditions," *Express Polymer Letters,* 3 (2009), 126-36.

5 Jean L Leblanc, "Rubber–Filler Interactions and Rheological Properties in Filled Compounds," *Progress in Polymer Science,* 27 (2002), 627-87.

6 Mark D Frogley, Diana Ravich, and H Daniel Wagner, "Mechanical Properties of Carbon Nanoparticle-Reinforced Elastomers," *Composites Science and Technology,* 63 (2003), 1647-54.

7 Gert Heinrich, and Manfred Klüppel, "Recent Advances in the Theory of Filler Networking in Elastomers," in Filled Elastomers Drug Delivery Systems, Springer, 2002, pp. 1-44.

8 M-J Wang, "Effect of Filler-Elastomer Interaction on Tire Tread Performance Part I Hysteresis of Filled Vulcanizates," *KGK. Kautschuk, Gummi, Kunststoffe,* 60 (2007), 438-43.

9 M-J Wang, "Effect of Filler-Elastomer Interaction on Tire Tread Performance Part Ii Effects on Wet Friction of Filled Vulcanizates," *KGK. Kautschuk, Gummi, Kunststoffe,* 61 (2008), 33-42.

10 AR Payne, and RE Whittaker, "Reinforcement of Rubber with Carbon Black," *Composites,* 1 (1970), 203-14.

11 D Qian, E Co Dickey, R Andrews, and T Rantell, "Load Transfer and Deformation Mechanisms in Carbon Nanotube-Polystyrene Composites," *Applied Physics Letters,* 76 (2000), 2868-70.

12 Hong‐Xia Jiang, Qing‐Qing Ni, and Toshiaki Natsuki, "Tensile Properties and Reinforcement Mechanisms of Natural Rubber/Vapor‐Grown Carbon Nanofiber Composite," *Polymer Composites,* 31 (2010), 1099-104.

13 James Lindsay White, Rubber Processing: Technology, Materials, and Principles Hanser Cincinnati, 1995.

14 Christopher P Toumey, "Reading Feynman into Nanotechnology," *Techné: Research in Philosophy and Technology,* 12 (2008), 133-68.

15 Norio Taniguchi, "On the Basic Concept of Nanotechnology," in *Proc. Intl. Conf. Prod. Eng. Tokyo, Part II, Japan Society of Precision Engineering,* 1974, pp. 18-23.

16 T Koyama, and M Endo, "Structure and Growth Process of Vapor-Grown Carbon Fibers," (1983).

17 Sumio Iijima, "Helical Microtubules of Graphitic Carbon," *Nature,* 354 (1991), 56-58.

18 Min-Feng Yu, Oleg Lourie, Mark J Dyer, Katerina Moloni, Thomas F Kelly, and Rodney S Ruoff, "Strength and Breaking Mechanism of Multiwalled Carbon Nanotubes under Tensile Load," *Science,* 287 (2000), 637-40.

19 S Bellucci, "Carbon Nanotubes: Physics and Applications," *Physica Status Solidi (c),* 2 (2005), 34-47.

20 Han Gi Chae, and Satish Kumar, "Rigid‐Rod Polymeric Fibers," *Journal of Applied Polymer Science,* 100 (2006), 791-802.

21 Michele Meo, and Marco Rossi, "Prediction of Young's Modulus of Single Wall Carbon Nanotubes by Molecular-Mechanics Based Finite Element Modelling," *Composites Science and Technology,* 66 (2006), 1597-605.

22 Susan B Sinnott, and Rodney Andrews, "Carbon Nanotubes: Synthesis, Properties, and Applications," *Critical Reviews in Solid State and Materials Sciences,* 26 (2001), 145-249.

23 BG Demczyk, YM Wang, J Cumings, M Hetman, W Han, A Zettl, and RO Ritchie, "Direct Mechanical Measurement of the Tensile Strength and Elastic Modulus of Multiwalled Carbon Nanotubes," *Materials Science and Engineering: A,* 334 (2002), 173-78.

24 Australian Stainless Steel Development Association (ASSDA), "Properties of Stainless Steel," 2006.

25 HD Wagner, Reinforcement Encyclopedia of Polymer Science and Technology, John Wiley & Sons, 2002.

26 RF Curl, RE Smalley, HW Kroto, JR Heath, and SC O'Brien, "C60: Buckminsterfullerene," *Nature,* 318 (1985), 2.

27 Jack B Howard, J Thomas McKinnon, Yakov Makarovsky, Arthur L Lafleur, and M Elaine Johnson, "Fullerenes C60 and C70 in Flames," *Nature,* 352 (1991), 139-41.

28 T.Y. Hughes, "Charles Roland Chambers," US Patents, 1889.

29 WR Davis, RJ Slawson, and GR Rigby, "An Unusual Form of Carbon," (1953).

30 TW Ebbesen, and PM Ajayan, "Large-Scale Synthesis of Carbon Nanotubes," *Nature,* 358 (1992), 220-22.

31 C Journet, WK Maser, P Bernier, A Loiseau, M Lamy de La Chapelle, de la S Lefrant, P Deniard, R Lee, and JE Fischer, "Large-Scale Production of Single-Walled Carbon Nanotubes by the Electric-Arc Technique," *Nature,* 388 (1997), 756-58.

32 Ting Guo, Pavel Nikolaev, Andreas Thess, DT Colbert, and RE Smalley, "Catalytic Growth of Single-Walled Manotubes by Laser Vaporization," *Chemical Physics Letters,* 243 (1995), 49-54.

33 M Jose‐Yacaman, M Miki‐Yoshida, L Rendon, and JG Santiesteban, "Catalytic Growth of Carbon Microtubules with Fullerene Structure," *Applied Physics Letters,* 62 (1993), 202-04.

34 M Chhowalla, KBK Teo, C Ducati, NL Rupesinghe, GAJ Amaratunga, AC Ferrari, D Roy, J Robertson, and WI Milne, "Growth Process Conditions of Vertically Aligned Carbon Nanotubes Using Plasma Enhanced Chemical Vapor Deposition," *Journal of Applied Physics,* 90 (2001), 5308-17.

35 Kenneth KS Lau, Jeffrey A Caulfield, and Karen K Gleason, "Structure and Morphology of Fluorocarbon Films Grown by Hot Filament Chemical Vapor Deposition," *Chemistry of Materials,* 12 (2000), 3032-37.

36 J Berzelius, "Isomerie, Unterscheidung Von Damit Analogen Verhältnissen," *Jahresberichte über die Fortschritte der physichen der Wissenschaften,* 12 (1833), 63-67.

37 Hermann Staudinger, "ber Polymerisation," *Berichte der deutschen chemischen Gesellschaft (A and B Series),* 53 (1920), 1073-85.

38 Jonathan N Coleman, Umar Khan, Werner J Blau, and Yurii K Gun'ko, "Small but Strong: A Review of the Mechanical Properties of Carbon Nanotube–Polymer Composites," *Carbon,* 44 (2006), 1624-52.

39 TM Junisbekov, Vladimir Nikolaevich Kestel′man, and NI Malinin, Stress Relaxation in Viscoelastic Materials, Science Pub Inc, 2003.

40 Cesana.com, Market Study on Synthetic Rubber, 2013.

41 Qinmin Pan, and Garry L Rempel, "Investigation of Fundamental Data for Nitrile Butadiene Rubber in Monochlorobenzene and O‐Dichlorobenzene," *Polymer Engineering & Science*, 44 (2004), 88-95.

42 Ting Li, "Catalytic Hydrogenation of Nitrile Rubber in High Concentration Solution," (2011).

43 Yoichiro Kubo, and Kiyomori Ohura, "Process for Hydrogenating Conjugated Diene Polymers," US Patents, 1990.

44 Hormoz Azizian, and Gary L Rempel, "Polymer Hydrogenation Process," US Patents, 1984.

45 NA Mohammadi, and GL Rempel, "Homogeneous Selective Catalytic Hydrogenation of C= C in Acrylonitrile-Butadiene Copolymer," *Macromolecules*, 20 (1987), 2362-68.

46 Ronald J Hoxmeier, and Lynn H Slaugh, "Hydrogenation Process," US Patents, 1989.

47 Ronald J Hoxmeier, "Hydrogenation Process," US Patents, 1990.

48 Lifeng Zhang, "Development of a Novel Continuous Process for Hydrogenation of Nbr," University of Waterloo, 2007.

49 Lifeng Zhang, Qinmin Pan, and Garry L Rempel, "Liquid Backmixing and Phase Holdup in a Gas-Liquid Multistage Agitated Contactor," *Industrial & Engineering Chemistry Research*, 44 (2005), 5304-11.

50 Lifeng Zhang, Qinmin Pan, and Garry L Rempel, "Liquid Phase Mixing and Gas Hold-up in a Multistage-Agitated Contactor with Co-Current Upflow of Air/Viscous Fluids," *Chemical Engineering Science,* 61 (2006), 6189-98.

51 Lifeng Zhang, Qinmin Pan, and Garry L Rempel, "Residence Time Distribution in a Multistage Agitated Contactor with Newtonian Fluids: Cfd Prediction and Experimental Validation," *Industrial & Engineering Chemistry Research,* 46 (2007), 3538-46.

52 Garry L Rempel, Qinmin Pan, and Jialong Wu, "Homogeneous Catalytic Hydrogenation of Polymers," *The Handbook of Homogeneous HydrogenaJUtion* (2006), 547-83.

53 JH Koo, "Polymer Nanocomposites: Processing, Characterization, and Applications. 2006," McGraw-Hill, New York, NY.

54 Pulickel M Ajayan, Linda S Schadler, and Paul V Braun, Nanocomposite Science and Technology John Wiley & Sons, 2006.

55 Gary G Tibbetts, and John J McHugh, "Mechanical Properties of Vapor-Grown Carbon Fiber Composites with Thermoplastic Matrices," *Journal of Materials Research,* 14 (1999), 2871-80.

56 K Lozano, and EV Barrera, "Nanofiber - Reinforced Thermoplastic Composites. I. Thermoanalytical and Mechanical Analyses," *Journal of Applied Polymer Science,* 79 (2001), 125-33.

57 AR Payne, "The Elasticity of Carbon Black Networks," *Journal of Colloid Science,* 19 (1964), 744-54.

58 Eugene Guth, "Theory of Filler Reinforcement," *Journal of Applied Physics*, 16 (1945), 20-25.